The study of the magnetization process of Fe film by magnetic Compton scattering and Mössbauer spectroscopy

Akane Agui[1], Ryo Masuda[2], Yasuhiro Kobayashi[2], Tadashi Kato[3], Shun Emoto[3], Kosuke Suzuki[3], and Hiroshi Sakurai[3]

[1]corresponding author's email: agui@spring8.or.jp

[1] *Quantum Beam Science Center, Japan Atomic Energy Agency, SPring-8, Sayo, Hyogo, 679-5148, Japan*

[2] *Research Reactor Institute, Kyoto University, Sennan, Osaka, 590-0494, Japan.*

[3] *Department of Electronics and Informatics, Gunma University, Kiryu, Gunma, 376-8515, Japan*

ABSTRACT

The magnetization process of Fe (110) film was investigated using the field dependence of magnetic Compton scattering and Mössbauer spectroscopy. The spin and orbital magnetic moment specific magnetization versus magnetizing field curves were obtained from the magnetic Compton profiles, and the angles between the magnetizing field and the magnetic moment, θ, were obtained from the Mössbauer spectra. It was found that the magnetizing field dependence of the ratio between orbital moment and spin moment was related to θ. We indicate that the magnetic field dependence of the orbital magnetic moment plays a role in the magnetization process.

Keywords: Fe film, Magnetic Compton scattering, Mössbauer spectroscopy, magnetization process

1. INTRODUCTION

Magnetic Compton scattering is a powerful tool for investigating magnetically active electrons, in particular 3d electrons in transition metals and 4f electrons in rare earth metals [1,2,3,4]. A Compton profile (CP) is represented by a double integral of the momentum density of electrons in momentum space. In the case of Fe, the magnetic Compton profile (MCP, $J_{mag}(p_z)$) is separated into the momentum distributions of 3d and 4s4p electrons because the momentum distribution of each electron is different. Magnetic Compton scattering has very unique characteristics; in particular, spin magnetic moment can be derived by integrating MCP. By applying this characteristics, 3d spin moment and 4s4p spin moment can be obtained separately, so that the microscopic magnetic state in the material can be studied. For example, Mizusaki et al. studied sp-like itinerant spin-polarized electrons in a Co-Heusler alloy and reported that the number of spin-polarized localized d electrons was proportional to the strength of the sp-d magnetic interaction [5].

We have developed a method for measuring spin moment selective magnetization (M) versus magnetizing field (H), to obtain spin-specific MH (SSMH) curve using the field dependence of MCP in combination with a conventional total magnetization curve measurement [6-10]. Moreover, building on this method, orbital moment specific MH (OSMH) curve and an element specific MH (ESMH) curve measurements have been successfully performed. For example, from MCP measurement of Tb-Co thin film, it was revealed that the spin magnetization of Tb 4f electrons had hard magnetism, whereas conduction magnetization was

soft [7]. This result shows that MCP is useful for investigating each characteristic of magnetically active 3d, 4f, and conduction electrons separately.

Mössbauer spectroscopy is a traditional element-selective method for studying magnetic materials. Mössbauer measurement is based on the resonant absorption of γ-rays by a nucleus affected by its surrounding electrons through hyperfine interactions. It is also a site-specific method for measuring atomic magnetic moment in combination with the valence, the ligand symmetry, so on. In particular, many studies have been reported on the electronic state of Fe, including its magnetic interaction and atomic magnetic moment [11].

In this study, we report the results from the magnetic field dependence of MCP and Mössbauer spectra measurements of Fe (110) film. Iron is a classical ferromagnetic material, and enormous research has been conducted from multilateral points of view over the course of several centuries [12]. Iron is an essential material from which various magnetic materials have been derived. Today, a detailed investigation of the magnetization process of Fe is important for both basic material science and industrial material development.

We will discuss the magnetization process of Fe from a microscopic view-point by Compton scattering and Mössbauer spectroscopy. The magnetization processes of spin and orbital moment will be discussed. The rest of this paper is organized as follows: after descriptions of the experiments in Section 2, we show in Section 3 our results for the MCPs and the Mössbauer spectra. Then, the magnetization process of Fe (110) film will be discussed in Section 4. The details of MCP analysis will be described in the Appendix.

2. EXPERIMENTAL

An Fe film (thickness: 5.0 μm) was deposited by RF sputtering (ULVAC MB96-1011)

onto an Al foil substrate (thickness: 12 μm) in Ar gas at a working pressure of 1.0 Pa. The film was covered by a Pd layer (thickness: 12 nm) to avoid oxidation. The structure was confirmed to have (110) texture by X-ray diffraction measurement using Cu $K\alpha_1$ radiation. The Al foil substrate was chosen to suppress background contributions from the substrate because Al has a high X-ray transmittance. A total magnetization curve measurement was performed using a superconducting quantum interference device (SQUID). The measurement was performed in perpendicular direction to the film at room temperature.

MCP measurements were conducted on beamline BL08W at SPring-8, Japan [13]. The emitted circularly polarized X-rays were monochromatized to 182.6 keV and focused on a spot of 1×0.8 mm^2 in area on the sample. The beam was parallel to the applied magnetic field, H = X T. The magnetic field, $0 < H < 2.5$ T, was applied perpendicular to the (110) film plane. To achieve a larger scattering volume, we prepared the specimen by stacking 32 sheets of the film. The scattered X-rays were detected by a 10-segment Ge solid-state detector (Canberra GL0115S) with a scattering angle of 178º. The overall momentum resolution was $\Delta p_z = 0.43$ au. The intensity of the incident beam was monitored using an Ar ion chamber for data normalization. The measurement was performed under vacuum at room temperature.

The magnetic field dependence of the Mössbauer spectra was observed by conventional methods using a radioactive source. γ-rays from ^{57}Co in the Rh matrix were transmitted through one sheet of the same Fe film at 250 K in vacuum with an external magnetic field. Then, they were detected by a proportional counter. The energy of the incident γ-rays were controlled by the velocity of the source combined with a velocity transducer. The velocity axis of the Mössbauer spectra was calibrated with α-Fe foil. The magnetic field was applied perpendicular to the film surface and the incident γ-rays were parallel to the magnetic field.

3. RESULTS

3.a Magnetic Compton profile

MCPs measured under several magnetic fields are shown in Fig. 1. All of them have a maximum intensity at 1.5 au and a long tail of approximately 10 au. The region of 0 au < p_z < 1.5 au is a valley. The difference between CP measured at magnetic field H = -X T and that at H = X T is represented as $J_{mag\_XT}(p_z)$. The definition of $J_{mag\_XT}(p_z)$ and other values are provided in the Appendix. The deviation of the MCP, given by the integral $\int \Delta J_{mag\_XT}(p_z)dp_z$, where $\Delta J_{mag\_XT}(p_z)$ is the difference between $J_{mag\_XT}(p_z)$ and $J_{mag\_2.5T}(p_z)$, is plotted in the top panel of Fig. 1 as a function of the magnetic field. $\int \Delta J_{mag\_XT}(p_z)dp_z$ is almost zero for each magnetic field, so the shape of MCP is the same under all magnetic fields. This means that the electron state contribution to the spin magnetic moment does not depend on the magnetic field.

3.b Mössbauer spectra

Figure 2, from top to bottom ,shows the Mössbauer spectra of Fe film while the magnetic field was first being enhanced, then reduced, then enhanced, and then reduced. A rough assessment shows that there are were changes which depended on the external magnetic field: the change of the absorption intensity at ±3 mm/s among the six absorptions due to the Zeeman split and the change of the strength of the hyperfine magnetic field at ±2.5 T. The field dependence of the absorption intensity at ±3 mm/s was analyzed by the difference in the direction of the Fe atomic magnetic moment. The angle between the γ-ray direction and the internal magnetic field, θ, was estimated from the intensity ratio using the following equation

[11]:

$$\frac{I_2}{I_3} = \frac{2}{1}\frac{2\sin^2\theta}{1+\cos^2\theta} \qquad (1)$$

where I_2 is the absorption intensity at ±3 mm/s and I_3 is that at ±0.8 mm/s. This estimation was based on the one site model, for simplicity.

4. DISCUSSION

In this section, we investigate the magnetization process of Fe film from the microscopic point of view. The solid circles in Fig. 3 (a) show the spin magnetic moment of Fe(110) film which was calculated from MCP measurements (see Appendix). This is the SSMH curve. The thick line in Fig. 3 (a) is the conventional total MH curve, which was measured by a SQUID at room temperature. The open squares show the OSMH curve, which was calculated by the subtraction of the SSMH curve from the total MH curve. Figure 3 (a) shows that the figure of the total MH curve is dominated by that of the SSMH curve. It also shows that the directions of the spin and that of orbital magnetic moments were the same.

The SSMH curve is re-plotted in Fig. 3(b) with solid circles. Assuming the total spin moment is the sum of the 3d component and the 4s4p component, the 3d spin and 4s4p spin moment components were separated (see Appendix). The open circles and the open diamonds show the 3d and 4s4p components, respectively. Figure 3(b) shows that the 3d spin moment dominated the total spin moment. In contrast, the direction of the 4s4p spin moment was opposite.

Figure 4 (a) shows the ratio of orbital moment to spin moment (O/S) and (b) shows ratio of 4s4p spin moment to 3d spin moment (4s4p/3d), both as functions of the magnetic field. The O/S was suppressed at approximately $|H|$ = 1.5 T and enhanced at approximately $|H|$ = 0 T

compared with its value at $|H|$ = 2.5 T. The 4s4p/3d had negative values, since the 4s4p spin moment coupled with the 3d spin moment antiferromagnetically. The 4s4p/3d did not depend on the magnetic field, as shown in Fig. 4(b). This is consistent with the fact that the electron state contribution to the spin magnetic moment does not depend on magnetizing field, as shown in the top panel of Fig. 1.

The averaged angle between the magnetic moment and external magnetizing field, θ, and the internal magnetic field were calculated from the Mössbauer spectra in Fig. 2. The definition of θ is illustrated in inset of Fig.5(a). If the magnetic moment is parallel or antiparallel to the magnetic field, θ is zero. θ and the internal magnetic field of Fe are plotted as functions of the magnetic field in Figs. 5(a) and (b), respectively. Since the angle θ was observed as eq.(1), θ was obtained from the average of $\cos^2\theta$ over the whole system. Although the total magnetization was a monotonically increasing function of the magnetic field (as shown in Fig. 3(a)), θ was not a monotonic function, as shown in Fig. 5(a). In the saturated field (i.e. $|H|$ = 2.5 T), θ was almost parallel or antiparallel to the magnetic field ($\theta = 8^{\circ}$), as shown in Fig. 5(a). With decreasing value of $|H|$, θ had maximal value of approximately 40° at approximately $|H|$ = 1 T and then decreased again to the value of 30° at H = 0 T. Thus, the magnetic moment did not lie in the film plane at H = 0 T. The internal field had an almost constant value of 33.2 T, which was the consistent with reported value of 33 T [13]. The Internal magnetic field decreased at approximately $|H| > 2$ T. This can be explained as follows. The internal field, H_N, at the nucleus had several terms associated with it:

$$H_N = H_S + H_L + H_D + (H - DM + \frac{4\pi}{3}M) \quad , \qquad (2)$$

where H was the external magnetic field, DM was the demagnetizing field, $4\pi M/3$ is the Lorentz field, H_S was the Fermi contact term, H_L was the orbital magnetic term, and H_D was the dipolar term. When the magnetization of the Fe film was not saturated, the demagnetization field, DM,

canceled out the external magnetic field, H. When the magnetization of the Fe film was saturated, the external magnetic field overcame the demagnetization field of Fe, and began to affect the internal field, H_N.

Here, we discuss the magnetization process of the spin magnetic moment. The shape of the MCP was the same under any magnetic field as shown in Fig. 1. The 4s4p/3d did not depend on the magnetic field as shown in Fig. 4(b). The internal magnetic field had an almost constant value of 33.2 T, which was consistent with the reported value of 33 T, as shown in Fig. 5(b). These results show that the electron state contribution to spin magnetic moment did not depend on the magnetic field. Kubo and Asano have well explained MCP at room temperature by theoretical calculation, namely 0 K [16]. We used their results in our discussion.

While the electron state contribution to the spin magnetic moment did not depend on the magnetic field, the O/S did, as shown in Fig. 4(a). This suggests that the orbital moment depended on the magnetic field. The orbital moment was suppressed at approximately $|H| = 1.5$ T and enhanced at approximately $|H| = 0$ T compared with its value at $|H| = 2.5$ T. Elmers et al. proposed that the contribution of the orbital magnetic moment of the Heusler Co_2FeAl compounds increased in a low magnetic field. In general, the orbital moment depends on the magnetization direction relative to the easy axis. The orbital magnetic moment is largest when the magnetization is directed along the easy axis of the magnetocrystalline or magnetoelastic anisotropy, while it is suppressed to some extent upon rotation toward the hard axis. Therefore, the orbital moment depends on the applied magnetic field [14]. Consequently, we assume that the magnetic field dependence of orbital moment had some correlation with θ, as shown Fig. 5(a). θ had maximum value of approximately 40° at approximately $|H| = 1$ T, and had a small value of 30° at $H = 0$ T. A small θ meant the magnetic moment was likely preferentially perpendicular to the film surface. With decreasing magnetic field, $|H|$ from 2.5 T, the magnetic

moment was oriented in the plane by demagnetization effect and crystalline magnetic anisotropy. With further decrease of the magnetic field to H = 0 T, the magnetic moment preferred to turn out from being in-plane to being oriented along the easy axis of (100), because the film had (110) texture and the easy axis was (100). In this paper, we represent the canting angle θ is the same for parallel and antiparallel to the applied magnetic field directions. The SQUID curve shows the behavior which dominated by mainly shape anisotropy. For detail, there are magnetic domains and magnetic domain walls. It is known that perpendicular magnetization components arise near magnetic domain walls and it makes canting angle θ as shown. So that, SQUID magnetization curve (Fig. 3(a)) is monotonic, but the Fe spin canting angle θ shows nonmonotonic behavior. Therefore, we indicate that the magnetic field dependence of the orbital magnetic moment played a role in the magnetization process.

In conclusion, we investigated the magnetization process of Fe (110) film. Using the magnetic field dependence of MCP, SSMH, OSMH, and ESMH curves were obtained, and the angle between the magnetic field and magnetic moment was obtained from Mössbauer spectra. They showed that the magnetizing field dependence of the ratio of orbital moment and spin moment were related to θ, i.e., this result suggests that orbital moment played key a role in changing θ. We indicate that the magnetic field dependence of the orbital magnetic moment played a role in the magnetization process.

Acknowledgement

The authors thank Mr. K. Hosoya, of Gunma University for his technical supports. We gratefully acknowledge Professor M. Seto for his help with Mössbauer spectroscopy measurements. The MCP experiments were performed with the approval of the Japan

Synchrotron Research Institute (JASRI), Proposal Nos. 2010A1458, 2011A1115, 2012B1235, 2012B1235, 2013B1132, and 2014B1121, International Research Center for Nuclear Materials Science, Institute of Material Research, Tohoku University, Proposal No. 11F0017, and HRCC of Gunma University, Proposal 2011-2012. This work was supported by JSPS KAKENHI 21560322 (Grant-in-aid for Scientific Research (C)), 24560364 (Grant-in-aid for Scientific Research (C)), and 24221005 (Grant-in-Aid for Scientific Research (S)).

Appendix

The MCP, $J_{mag}(p_z)$, is defined as,

$$J_{mag}(p_z) = \iint (n_{maj}(\boldsymbol{p}) - n_{min}(\boldsymbol{p}))dp_x dp_y. \quad \text{(a.1)}$$

Here, $\boldsymbol{p}(p_x, p_y, p_z)$ is the momentum, and $n_{maj}(\boldsymbol{p})$ and $n_{min}(\boldsymbol{p})$ are the electron momentum densities of the majority and minority spins, respectively [1-4]. The spin magnetic moment, μ_s, is equal to the area under $J_{mag}(p_z)$,

$$\mu_s = \int J_{mag}(p_z)dp_z. \quad \text{(a.2)}$$

The difference between the CP measured under a magnetic field of H = -X T from that measured under a magnetic field of H = X T is represented as $J_{mag\_X\,T}(p_z)$.

Kubo and Asano [16] calculated the MCPs of the 3d and 4s4p electron states of Fe using the full-potential linearized augmented plane wave method and reported that the 3d electron state covered the region of 0 au < p_z < 8 au, while the 4s4p state was localized in the region of 0 au < p_z < 2 au.

The intensity of MCP in the region between 2 au and 10 au changed as a function of the magnetic field, while the shape stayed the same. This means that the MCP measure at H = X T, $J_{mag\_X\,T}(p_z)$, was described by the shape of $J_{mag\_2.5T}(p_z)$ in 2 au < p_z < 10 au with a

scale factor of a. Using a as a fitting parameter for the region in 2 au < p_z < 10 au, the residual remaining in p_z < 2 au, $\Delta J_{mag\_X\,T}(p_z)$, could be defined as follows:

$$\Delta J_{mag\_X\,T}(p_z) = J_{mag\_X\,T}(p_z) - aJ_{mag\_2.5\,T}(p_z). \qquad \text{(a.3)}$$

The spin magnetic moment at H = 2.5 T, $\mu_{2.5\,T}$, was calculated as the area under $J_{mag\_2.5\,T}(p_z)$ and, considering the existence of the magnetically active electrons, $\mu_{2.5\,T}$ could be defined as the summation of the spin magnetic moment of 3d electrons at H = 2.5 T, $\mu_{2.5\,T\_3d}$, with that of 4s4p, $\mu_{2.5\,T\_4s4p}$ as follows:

$$\mu_{2.5\,T} = \int J_{mag\_2.5\,T}(p_z)dp_z = \mu_{2.5\,T\_3d} + \mu_{2.5\,T\_4s4p}. \qquad \text{(a.4)}$$

It is known the magnetization of Fe film becomes saturated at 2.15 T perpendicular to the surface. Kubo and Asano [15] reported that the saturation magnetizations of 3d and 4s4p electrons in Fe were 2.205 μ_B and -0.135 μ_B, respectively. Thus, that the total saturate magnetization of Fe was calculated to be 2.07 μ_B.

In an analogous way, the spin magnetic moment at H = X T, $\mu_{X\,T}$, was calculated from the MCP at H = X T, $J_{mag\_X\,T}(p_z)$, and could be defined as the summation of the spin magnetic moment of a 3d electron at X T, $\mu_{X\,T\_3d}$ with and that of a 4s4p electron, $\mu_{X\,T\_4s4p}$, as follows:

$$\mu_{X\,T} = \int J_{mag\_X\,T}(p_z)dp_z = \mu_{X\,T\_3d} + \mu_{X\,T\_4s4p}. \qquad \text{(a.5)}$$

Integrating both sides of eq. (a.3) and substituting eqs (a.4) and (a.5) as follows, we obtained:

$$\begin{aligned}\int \Delta J_{mag\_X\,T}(p_z)dp_z &= \int J_{mag\_X\,T}(p_z)dp_z - a\int J_{mag\_2.5T}(p_z)dp_z \\ &= \mu_{XT\_3d} + \mu_{XT\_4s4p} - a(\mu_{2.5T\_3d} + \mu_{2.5T\_4s4p}) \\ &= (\mu_{XT\_3d} - a\mu_{2.5T\_3d}) + (\mu_{XT\_4s4p} - a\mu_{2.5T\_4s4p}) \qquad \text{(a.6)}\end{aligned}$$

Assuming that $\mu_{XT\_3d} - a\mu_{2.5T\_3d} = 0$ as a result of the fitting, the spin magnetic moment of 3d and 4s4p at H = X T could be calculated using eqs (a.7) and (a.8), respectively.

$$\mu_{XT\_3d} = a\mu_{2.5T\_3d} \qquad \text{(a.7)},$$

$$\mu_{\mathrm{XT\_4s4p}} = \int \Delta J_{mag\_\mathrm{XT}}(p_z)dp_z + a\mu_{\mathrm{2.5T\_4s4p}} \quad \text{(a.8)}.$$

References

[1] M. J. Cooper, P. E. Mijnarends, N. Shiotani, N. Sakai, and A. Bansil, *X-ray Compton Scattering* (Oxford University Press, Oxford, 2004).

[2] M. J. Cooper, E. Zukowski, S. P. Collins, D. N. Timms, F. Itoh, and H. Sakurai, J. Phys. Condens. Matter **4**, L399 (1992).

[3] P. Carra, M. Fabrizio, G. Santoro, and B. T. Thole, Phys. Rev. B **53**, R5994 (1996).

[4] N. Sakai, J. Appl. Crystallogr. **29**, 81 (1996).

[5] S. Mizusaki, T. Ohnishi, T. C. Ozawa, Y. Noro, M. Itou, Y. Sakurai, and Y. Nagata, J. Appl. Phys. **111**, 063915 (2012).

[6] A. Agui, H. Sakurai, T. Tamura, T. Kurachi, M. Tanaka, H. Adachi, and H. Kawata, J. Synchrotron Rad. **17**, 321 (2010).

[7] A. Agui, S. Matsumoto, H. Sakurai, N. Tsuji, S. Homma, Y. Sakurai, and M. Itou, Appl. Phys. Express **4**, 083002 (2011) .

[8] A. Agui, T. Unno, S. Matsumoto, K. Suzuki, A. Koizumi, and H. Sakurai, J. App. Phys. **114**, 183904 (2013).

[9] T. Kato, K. Suzuki, S. Takubo, Y. Homma, M. Itou, Y. Sakurai, and H. Sakurai, Applied Mechanics and Materials, **423-426**, 271 (2013).

[10] K. Suzuki, S. Takubo, T. Kato, M. Yamazoe, K. Hoshi, Y. Homma, M. Itou, Y. Sakurai, and H. Sakurai, Appl. Phys. Lett. **105**, 072412 (2014).

[11] Ed: U. Gonser, *Mössbauer spectroscopy* (Springer-Verger Berlin Heidelberg New York 1975).

[12] Ed: R. M. Bozorth, *Ferromagnetism* (An IEEE press New York 1951), in particular Chapter 10.

[13] Y. Kakutani, Y. Kubo, A. Koizumi, N. Sakai, B. L. Ahuja, and B. K. Sharma, J. Phys. Soc. Jpn. **72**, 599 (2003).

[14] C. E. Violet and D. N. Pikorn, J. Appl. Phys. **42**, 4339 (1971).

[15] H. J. Elmers, S.Wurmehl, G. H. Fecher, G. Jakob, C. Felser, and G. Schöhnense, Appl. Phys. A **79**, 557 (2004).

[16] Y. Kubo and S. Asano, Phys. Rev. B **42**, 4431 (1990).

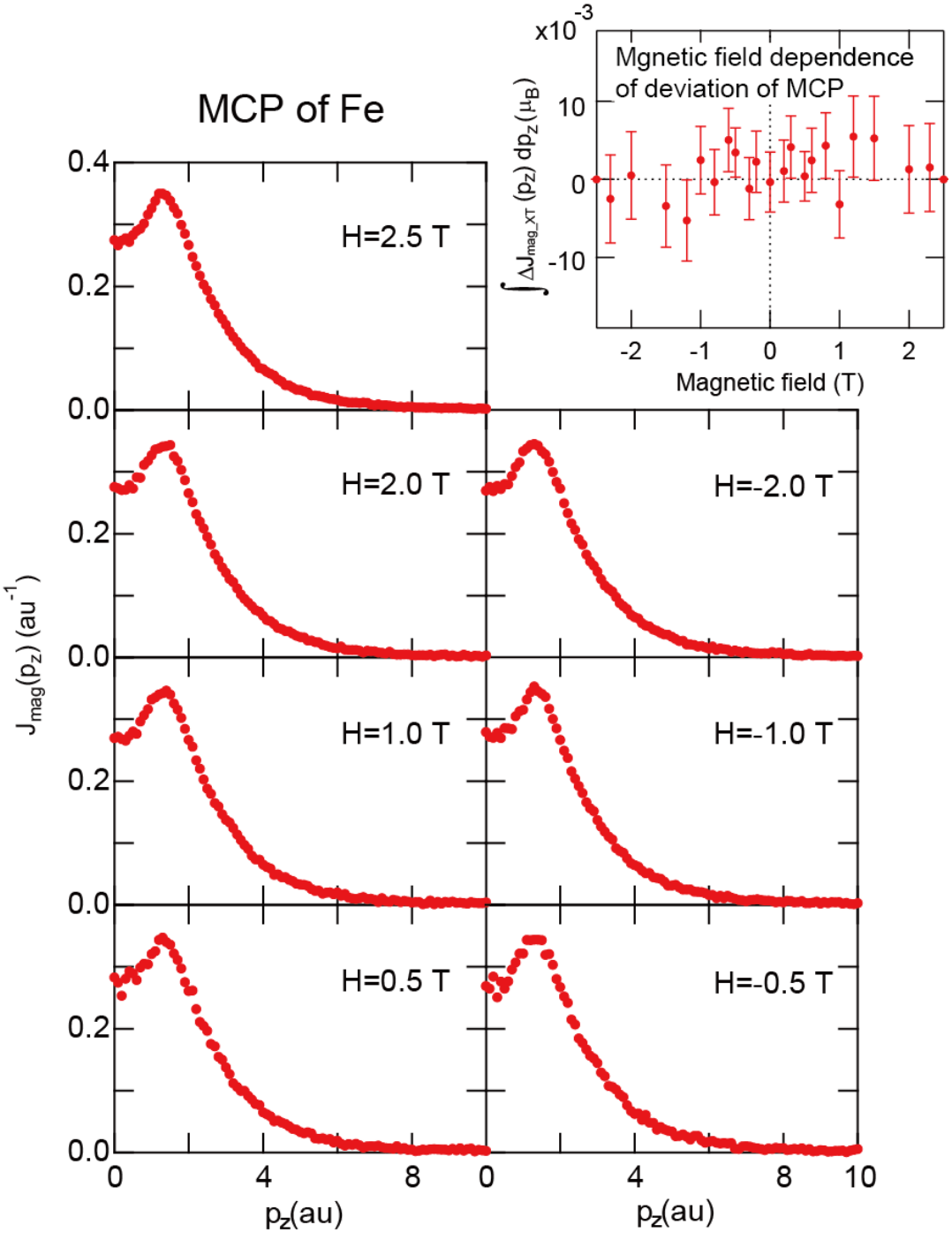

Figure 1: Magnetic Compton profile of Fe film at room temperature. Top right: Magnetic field dependence of the deviation of MCP, $\int \Delta J_{mag\_XT}(p_z)\mathrm{d}p_z$.

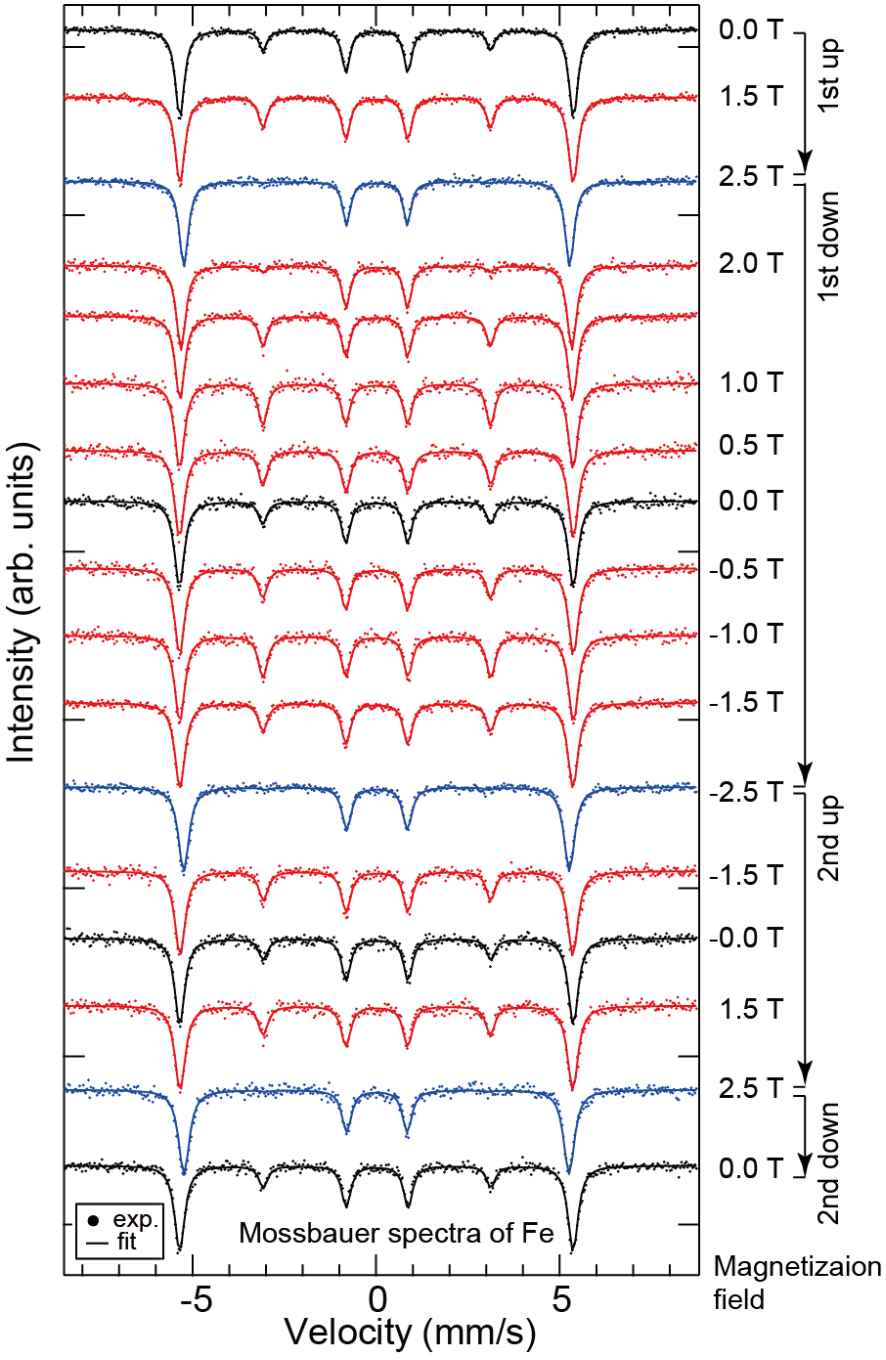

Figure 2: Applied magnetic field dependence of the Mössbauer spectra of Fe.

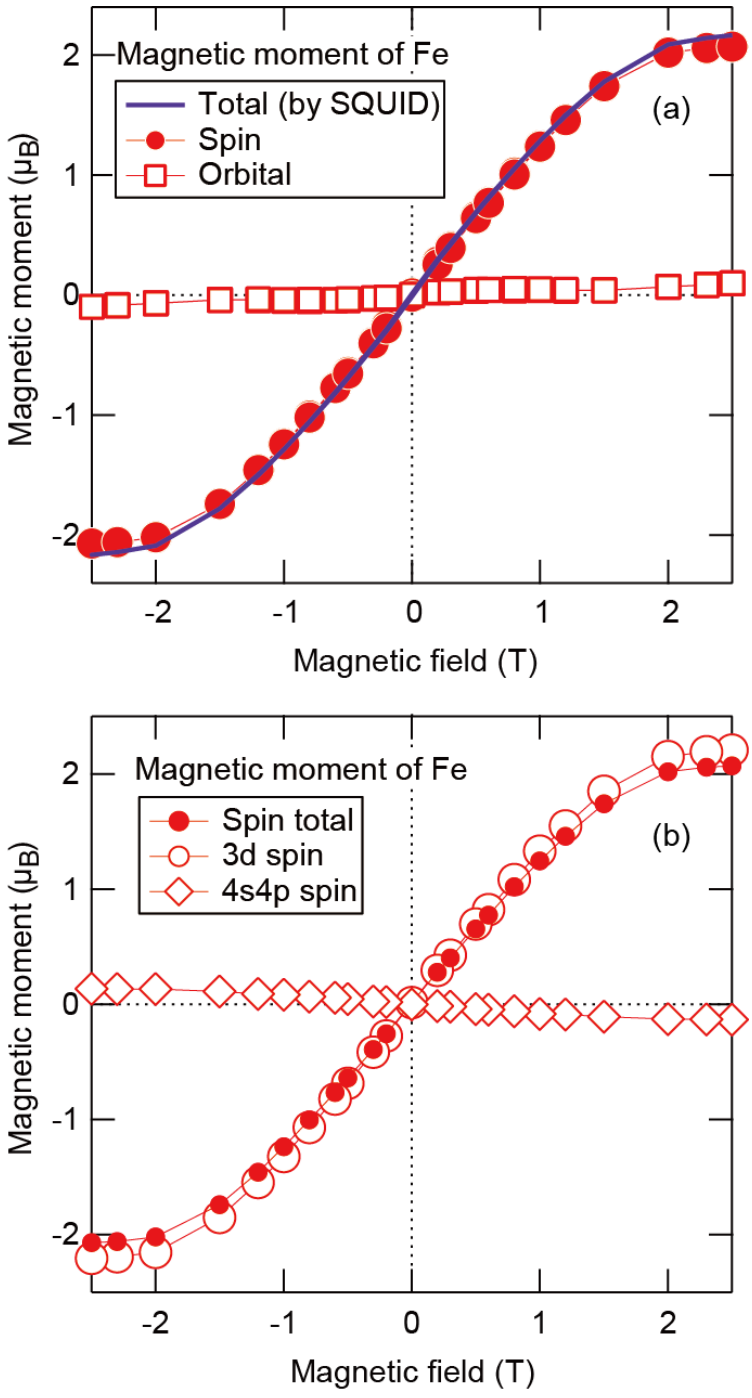

Figure 3: (a) ●: The spin magnetic moment of Fe (110) film which is the spin specific magnetization versus magnetizing field (SSMH) curve. -: the conventional total magnetization curve which was measured by SQUID. □: the orbital specific magnetization versus magnetizing field (OSMH) curve. (b) ●: SSMH, ○: 3d and ◇: 4s4p component.

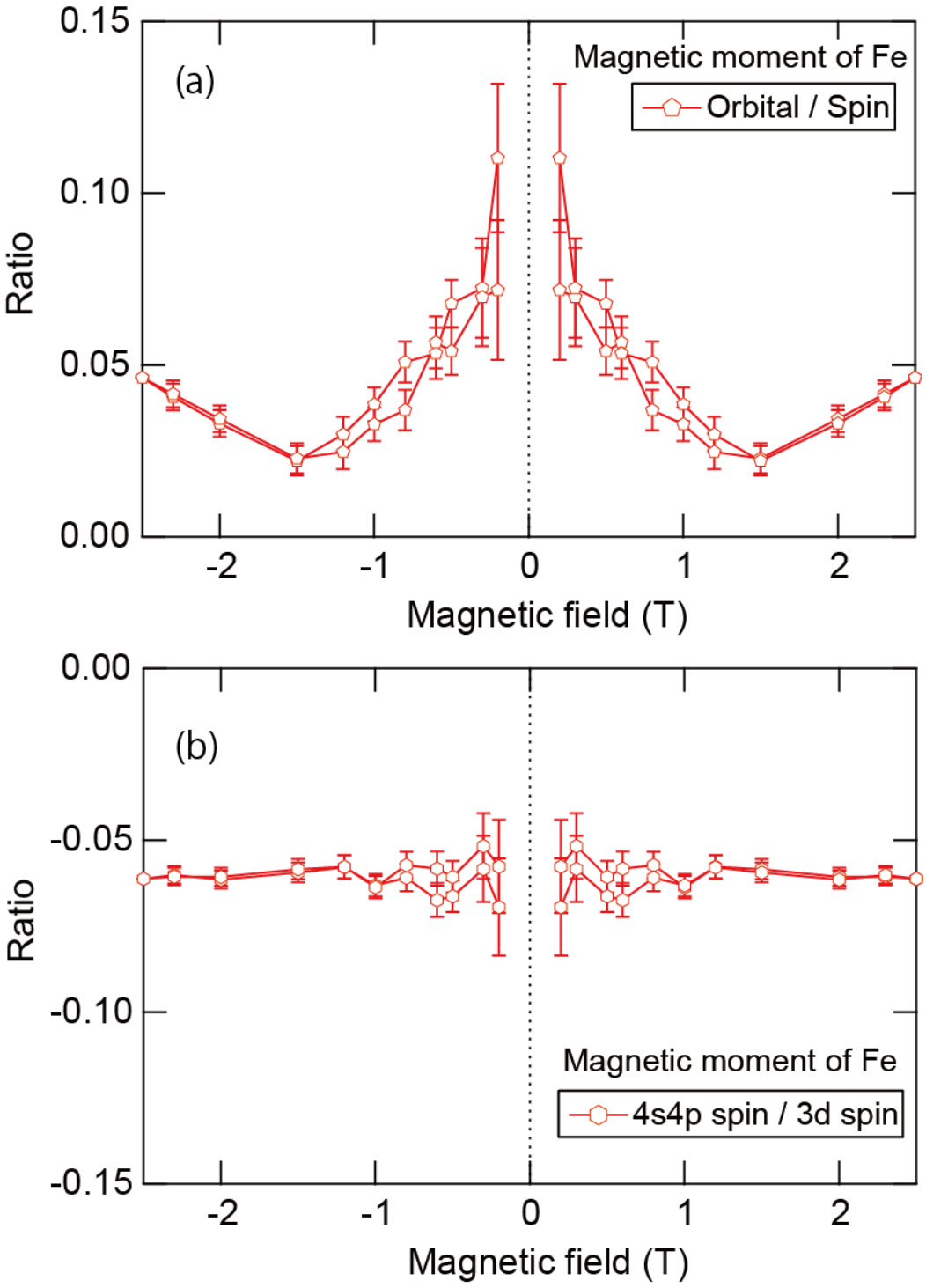

Figure 4: (a) The ratio of orbital moment to spin moment. (b) The ratio of 4s4p spin moment to 3d spin moment. The value at $H = 0$ T is not shown since its error bar is huge.

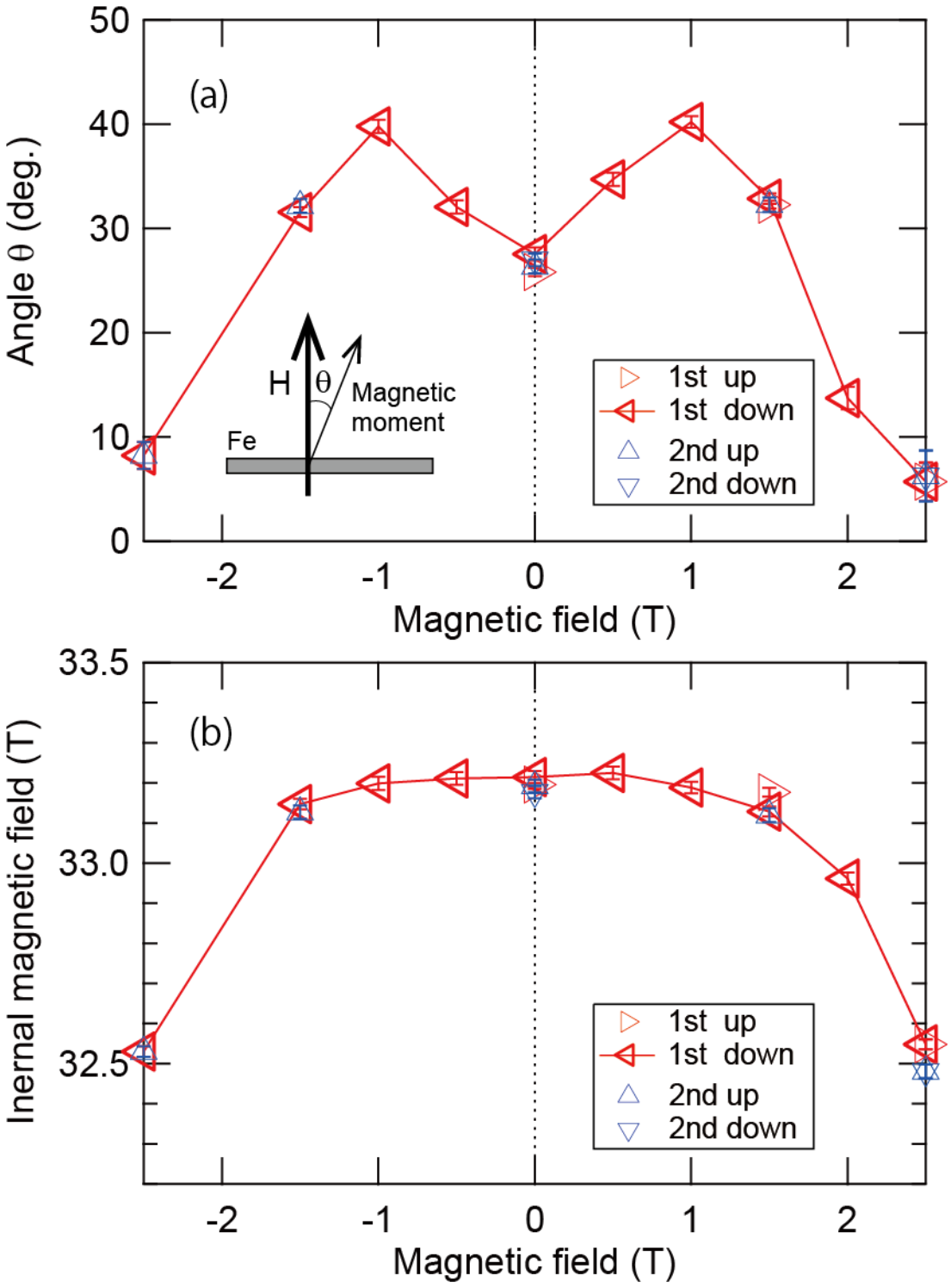

Figure 5: (a)The angle between the magnetic moment and the external magnetic field, θ, in Fe. Inset: The definition of θ. (b) The internal magnetic field in Fe.